Calibration Sets for Multiprimary Displays: Representation, Visualization, and Applications

Carlos Eduardo Rodríguez-Pardo, Gaurav Sharma
ECE Dept. Univ. of Rochester, Rochester, NY 14627-0126

Abstract

In this paper, we consider idealized additive multiprimary displays and provide: (a) a complete mathematical characterization for the calibration set*, i.e., the set of control values that produce a given color, (b) a subspace decomposition of the device control space that decomposes the control signals into constrained and unconstrained dimensions, and (c) a method for visualizing and analyzing alternative calibration strategies via the representation and the subspace decomposition. Specifically, we demonstrate that the calibration set for a given color is a convex polytope in the device control space whose vertices correspond to alternative tessellations of the gamut in a previously proposed representation. For a K primary display, we decompose the K dimensional control space into a* 3 *dimensional* control visual subspace *(CVS) that is completely determined by the desired color and a* $(K-3)$ *dimensional* control black space *(CBS) that contains the alternative calibrations within its linear varieties, i.e., affine translations. We use these results for ready visualization and analysis of these sets and of alternative calibration strategies for multiprimary displays. For display technologies such as OLED, where power is switched at the individual pixel level, our methodology reduces the minimum and maximum power calibration strategies to linear programs on polytopes, which are well-studied and allow corresponding calibrations to be immediately determined as appropriate vertices of the polytopes for calibration sets. The visualizations confirm the intuition that these calibration strategies are not necessarily well-behaved in the presence of device variability we highlight how alternative strategies can be formulated within the proposed framework.*

1 Introduction

Recent years have seen significant research on multiprimary color displays motivated largely by the desire for a larger color gamut. A variety of design methodologies have been proposed for the selection of primaries for these systems based on optimization of gamut-based display performance metrics [1–5]. In addition to the wider gamut capabilities, researchers have also explored other benefits of multiprimary displays, focusing on reduced power consumption [6, 7], improved the viewing angle [8] and higher resolution for rendered imagery [9, 10].

Because multiprimary display systems use a number of primaries greater than the minimum of three that is necessary for trichromatic matching of human perception, colors inside the display gamut can be obtained by the use of multiple alternative combinations of the primaries. Thus a fundamental step for color reproduction in multiprimary displays is to resolve this ambiguity through the selection of a *calibration*, i.e., a specific combination of primaries, for reproducing each color within the gamut. Although multiple calibration choices yield the same color, they typically differ with regard to other aspects of display performance. For instance, in organic light emitting diode (OLED) and other similar displays, where power is controlled for individual primaries at the pixel level, alternative calibrations differ in their power, which can form a basis for the selection between alternative calibrations. In the presence of inevitable device and observer variations, it is also necessary to ensure smoothness of the calibration across color space and this is usually an important criteria in the selection between alternative options for calibration.

Although several methodologies for calibration selection have been proposed for multiprimary displays [11–13], a complete characterization of the set of possible calibrations has not been previously considered, mostly due to the lack of a theoretical framework for the representation of general multiprimary display systems. Recent work has partly addressed this issue: a useful geometrical representation for the gamut for multiprimary displays as the union of disjoint parallelepipeds has recently been independently developed by two different groups with different motivations and approaches. Specifically, this representation is developed in [14] for efficient computation of gamut volumes in perceptual color spaces and in [15] for the purpose of color calibration for multiprimary display systems, although, both works also consider other aspects. In this paper, building upon this representation, we provide a complete mathematical characterization for the set of possible calibrations for a multiprimary display system and an attractive methodology for visualizing and analyzing these calibrations via a suitably chosen subspace decomposition of the display control space. In particular, we show that the set of calibrations is a convex polytope in the display control space with vertices corresponding to the alternatives for our previously proposed gamut representation in [14].

To allow for better visualization and analysis of alternative calibrations, we also propose a subspace decomposition of the display control space. Specifically, for a K primary display, we decompose the K dimensional control space into a 3 dimensional *control visual subspace* (CVS) that is completely determined by the desired color and a $(K-3)$ dimensional *control black space* (CBS) that completely contains the sets of alternative calibrations within its translates (formally, linear varieties). Calibration sets and alternative calibrations can therefore be visualized and analyzed in the CBS. As an application of out results, we demonstrate that minimal and maximal power calibrations are readily obtained using our framework and that the CBS provides an effective way to visualize and analyze properties of these and other alternative calibration strategies. For multiprimary display designs obtained in [5] our visualizations also show that the minimum and

maximum power calibration strategies are not particularly well-behaved in the presence of device and observer variability and that alternative formulations are therefore necessary for practical systems.

The rest of the paper is organized as follows. Section 2 introduces the display model and the geometrical representation for the gamut of multiprimary displays initially formulated in [14]. We use this representation in Section 3 to provide the convex polytope characterization for the set of calibrations. In Section 4 we motivate and develop the subspace decomposition of the display control space and show how calibration sets can be completely represented and visualized in the CBS. In Section 5, we show how minimal and maximal power calibrations can be formulated and readily solved using the proposed calibration set representation. In Section 6, we demonstrate applications of the framework to multiprimary designs with $K = 4, 5$, and 6 primaries and particularly demonstrate visualizations of alternative calibrations. We discuss the results and conclude in Section 7. To keep the material accessible, we defer formal mathematical proofs to a separate manuscript [16] and focus here on the results and implications, particularly emphasizing visual presentation designed to aid intuition.

2 Display Model and Gamut Representation in Multiprimary Systems

2.1 Display Model

For a system with K primaries, following closely the notation in [14], we denote by $p_i(\lambda)$ the spectral power density for the primary $i, 1 \leq i \leq K$. The intensity of the i^{th} primary is controlled independently by a corresponding control value $\alpha_i, 0 \leq \alpha_i \leq 1$, and the control vector $\alpha = [\alpha_1, \alpha_2, \ldots, \alpha_K]^T$ summarizes the full set of display control values. The display spectra $s(\lambda)$ corresponding to the control input α is then obtained as

$$s(\alpha;\lambda) = \sum_{i=1}^{K} \alpha_i p_i(\lambda) + s_0(\lambda), \tag{1}$$

where $s_0(\lambda)$ is the display black spectral radiance, which is the display emission when the intensities is set to zero $\alpha_i = 0, i \leq K$. A colorimetric representation can be obtained by computing the tristimulus coordinates in the CIE XYZ color space [17] for each of the primaries and the black spectra, which are denoted, respectively, by $\mathbf{p}_i$ and $\mathbf{t}_0$, where $\mathbf{p}_i = [p_{i,x}, p_{i,y}, p_{i,z}]^T$ and $\mathbf{t}_0 = [t_{0,x}, t_{0,y}, t_{0,z}]^T$.

In this manner, the tristimulus vector $\mathbf{t} = [t_x, t_y, t_z]^T$ for the spectra emitted by the display in response to the control input α, can be computed as

$$\begin{aligned} \mathbf{t}(\alpha) &= \sum_{i=1}^{K} \alpha_i \mathbf{p}_i + \mathbf{t}_0(\lambda), \\ &= \mathbf{P}\alpha + \mathbf{t}_0, \end{aligned} \tag{2}$$

where $\mathbf{P}$ represents the $3 \times N$ primary matrix $\mathbf{P} = [\mathbf{p}_1, \mathbf{p}_2, \ldots, \mathbf{p}_K]$. We assume throughout our development that $\mathbf{P}$ is non-degenerate in the sense that any selection of three columns from $\mathbf{P}$ is linearly independent.

The *forward model* presented in (2) is used to predict the color that a device reproduce, given a set of primary control values. The *backward model* also plays a fundamental role in the process of color reproduction. For given a color $\mathbf{t}$, the backward model determines the primary control vector α that is required to drive the display to be able to reproduce $\mathbf{t}$. In this process the value $\alpha(\mathbf{t})$ is usually known as a *calibration* for color $\mathbf{t}$.

In the three primary scenario, the backward and forward models are uniquely determined one from the other by the use of matrix inversion. In a multiprimary display, the system of equations in (2) is under-determined, and therefore, multiple solutions may be possible.

2.2 Geometrical Gamut Representation

Based on the forward model presented in (2), the display gamut, denoted by $\mathscr{G}_{\mathbf{P}}^{XYZ}$, is defined as the set that contains all the colors that the device is able to reproduce, can be expressed as,

$$\mathscr{G}_{\mathbf{P}} \quad = \quad \left\{ \mathbf{t} = \mathbf{P}\alpha | \alpha \in [0,1]^K \right\}, \tag{3}$$

where $[0,1]^K$ is the unitary hypercube in R^K. Using the geometrical properties of the gamut, and following closely the notation in [14], an alternative gamut representation can be formulated as the union of disjoint[1] parallelepipeds $\mathscr{P}$. Each of these geometrical objects can be interpreted as the gamut of an hypothetical three primary system, whose primaries are chosen from the original K primaries, and whose display black tristimulus is a binary combination of the remaining $K-3$ primaries. Since there are $\binom{K}{3}$ different ways of selecting a set three primaries, represented here by the 3×3 matrix $\mathbf{P}_j$, $j = 1, \ldots, \binom{K}{3}$, there are $\binom{K}{3}$ different parallelepipeds $\mathscr{P}_j$, and thus, the gamut can be expressed as [14],

$$\mathscr{G}_{\mathbf{P}} = \bigcup_{j=1}^{\binom{K}{3}} \mathscr{P}_j, \tag{4}$$

where $\mathscr{P}_j = \mathscr{G}_{\mathbf{P}_j} + \mathbf{t}_j + \mathbf{t}_0$ is the gamut of a three primary system with primary matrix $\mathbf{P}_j$, and black tristimulus $\mathbf{t}_j + \mathbf{t}_0$. The primaries in $\mathbf{P}_j$ are selected from the primaries in $\mathbf{P}$, while the *displacement vector* $\mathbf{t}_j$ is expressed as the binary combination (ones and zeros as coefficients) of the remaining $K-3$ primaries in $\mathbf{P}$ that are not present in $\mathbf{P}_j$. As a running example through the rest of our development, we will consider a display system with the primaries

$$\begin{aligned} \mathbf{P} \quad &= \quad [\mathbf{p}_1, \mathbf{p}_2, \mathbf{p}_3, \mathbf{p}_4] \\ &\stackrel{\text{def}}{=} \quad \begin{bmatrix} 0.3630 & 0.1539 & 0.0471 & 0.0758 \\ 0.1761 & 0.3700 & 0.3093 & 0.0244 \\ 0.0027 & 0.0179 & 0.1853 & 0.4415 \end{bmatrix}, \end{aligned} \tag{5}$$

which correspond to spectral power densities are shown in Fig. 1.

Assuming that the system described above has a zero black radiation, that is $\mathbf{t}_0 = \mathbf{0}$, the display gamut is shown in Fig. 2(a), where it can be appreciated that the gamut can be partitioned, or *tessellated* using four parallelepipeds, shown in Figs. 2(c)-2(f), each of them constructed from the selection of three primaries.

In particular, the tessellation depicted in Fig. 2(a) is obtained by placing first the parallelepiped formed by primaries $[\mathbf{p}_1, \mathbf{p}_2, \mathbf{p}_3]$

[1] The term "disjoint" is used to denote that the intersection between two parallelepipeds has a zero volume, i.e., the intersection is either empty, or includes either a face, or an edge, or a vertex.

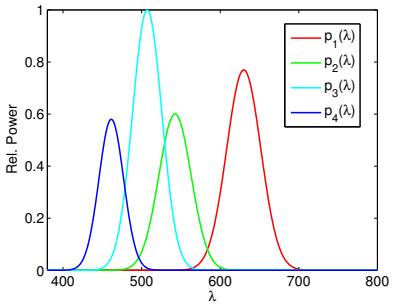

(a) Relative spectra power distribution

Figure 1. *Spectra power densities for the display system with primaries defined in* (5).

(Fig. 2(c)). The rest of parallelepipeds, which involve the remaining primary $\mathbf{p}_4$ (Figs. 2(e)- 2(f)), are displaced from the origin by a binary addition of the remaining primary, and the union of all parallelepipeds is the display gamut.

The representation provided in (4), however, is not unique. Figure 2(b) shows an alternative tessellation for the system introduced in (5), by placing first the parallelepiped in Fig. 2(d) build from primaries $[\mathbf{p}_2, \mathbf{p}_3, \mathbf{p}_4]$, and then adding the rest of the parallelepipeds that involve $\mathbf{p}_1$.

3 Calibrations and Calibration Sets

A calibration α for color $\mathbf{t}$ is a primary control vector that satisfies (2). In the three primary case, the calibration is unique. For the general scenario, we denote the set of calibrations for color $\mathbf{t} \in \mathscr{G}$ by $\Omega(\mathbf{t})$, which can be expressed as,

$$\Omega(\mathbf{t}) = \left\{ \alpha \in [0,1]^K \,\middle|\, \mathbf{t} = \mathbf{P}\alpha + \mathbf{t}_0 \right\}. \tag{6}$$

The geometrical gamut representation introduced in (4) offers a simple way to obtain elements in the calibration set. In fact, for every color it is possible to find a unique set of control values associated with each particular gamut representation. Specifically, for a given color $\mathbf{t} \in \mathscr{G}$ and a given gamut tessellation, there exists a parallelepiped $\mathscr{P}_j$, $j \leq \binom{K}{3}$ such that $\mathbf{t} \in \mathscr{P}_j$. Let denote by $\mathbb{P}_j$ the sequence of indexes of the primaries involved in the construction of the matrix $\mathbf{P}_j$, and by $\mathbb{T}_j$ the sequence of indexes of the primaries with nonzero coefficients in the binary combination that defines the displacement vector $\mathbf{t}_j$. The calibration associated with the given tessellation is denoted by ω, which vector entries are computed as,

$$\begin{aligned} \omega_{\mathbb{P}_j} &= \mathbf{P}_j^{-1}\left(\mathbf{t} - \mathbf{t}_j - \mathbf{t}_0\right), \\ \omega_{\mathbb{T}_j} &= 1, \\ \omega_{\sim\{\mathbb{P}_j,\mathbb{T}_j\}} &= 0, \end{aligned} \tag{7}$$

where the subscript $\sim \{\mathbb{P}_j, \mathbb{T}_j\}$ denotes the indexes for the primaries that are not actively involved in the definition of $\mathbf{P}_j$ or $\mathbf{t}_j$.

As an example, consider the color $\mathbf{t} = [0.2447, 0.4995, 0.3393]^T$ to be displayed by the system (5). Figures 3(a) and 3(b) show the parallelepipeds involved in the computation of the calibration for each of the two tessellations already introduced in Fig. 2. The table included in Fig. 3(c)

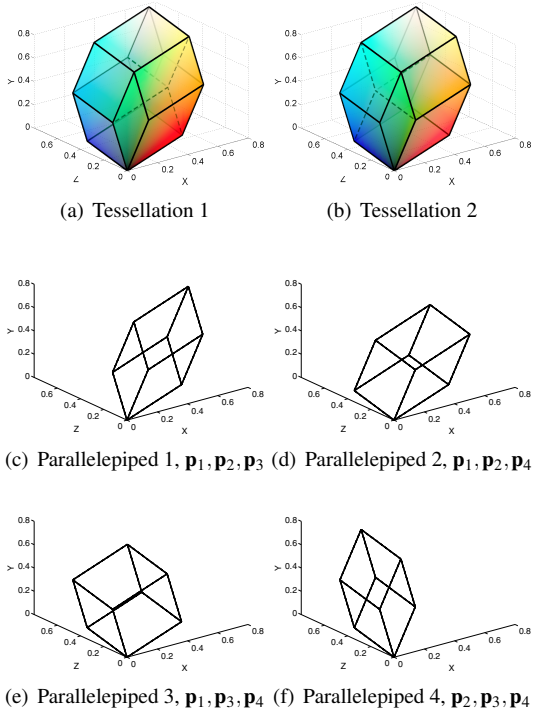

(a) Tessellation 1 (b) Tessellation 2

(c) Parallelepiped 1, $\mathbf{p}_1, \mathbf{p}_2, \mathbf{p}_3$ (d) Parallelepiped 2, $\mathbf{p}_1, \mathbf{p}_2, \mathbf{p}_4$

(e) Parallelepiped 3, $\mathbf{p}_1, \mathbf{p}_3, \mathbf{p}_4$ (f) Parallelepiped 4, $\mathbf{p}_2, \mathbf{p}_3, \mathbf{p}_4$

Figure 2. *Gamut representation for the system with four primaries $\mathbf{p}_1, \mathbf{p}_2, \mathbf{p}_3, \mathbf{p}_4$ defined in* (5) *and zero black radiance $\mathbf{t}_0 = \mathbf{0}$. (a) and (b) represent the display gamut tessellated in two different ways. Each tessellation is obtained by the displacement of the four parallelepipeds shown in (c), (d), (e) and (f), which represent the three primary gamuts for all $\binom{4}{3} = 4$ selections of* 3 *primaries from the set of* 4 *primaries.*

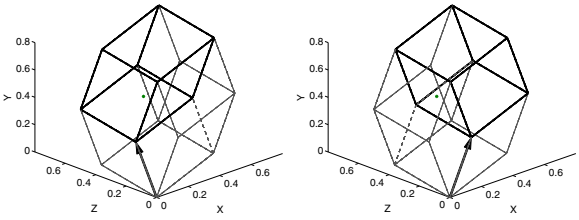

(a) Tessellation 1 (b) Tessellation 2

	Tessellation 1	Tessellation 2
$\mathbf{P}_j$	$[\mathbf{p}_1, \mathbf{p}_2, \mathbf{p}_4]$	$[\mathbf{p}_1, \mathbf{p}_3, \mathbf{p}_4]$
$\mathbf{t}_j$	$\mathbf{p}_3$	$\mathbf{p}_2$
$\mathbb{P}_j$	$[1,2,4]$	$[1,3,4]$
$\mathbb{T}_j$	$[3]$	$[2]$
$\omega(\mathbf{t})$	$[1/3, 1/3, 1, 1/3]^T$	$[0.084, 1, 0.592, 0.324]^T$

(c) Indices and numerical values

Figure 3. *Tessellated calibrations for $\mathbf{t} = [0.2447, 0.4995, 0.3393]^T$. Figures 3(a) and 3(b) shows,for each of the two possible tessellations, the geometrical elements that define the calibration for $\mathbf{t}$: the parallelepiped based on a 3×3 matrix $\mathbf{P}_j$, and a displacement vector $\mathbf{t}_j$. Corresponding indices and numerical values are shown in the tabulation in 3(c).*

shows the numerical values for the calibration vectors, and the corresponding parallelepiped matrix $\mathbf{P}_j$ and displacement vector $\mathbf{t}_j$.

The number of different tessellations depends on the characteristics of the primary set. A particular tessellation can be obtained by first selecting a set of three primaries, from $\binom{K}{3}$ possibilities. The rest of the primaries can be ordered in $(K-3)!$ different fashions, and thus, the gamut can be constructively obtained by adding the parallelepipeds that involve the remaining primaries, leaving $\frac{K!}{3!} = \binom{K}{3}(K-3)!$ ways to do it, or potentially $\frac{K!}{3!}$ different tessellations. A detailed constructive methodology for obtaining gamut representations is described in [16]. For the case of the primaries defined in (5), once considering all four possibilities of tessellating the gamut, only two of them are actually different, and they are the ones depicted in Figs. 2(a) and 2(b).

We denote by ω^i the calibration obtained by the i^{th} tessellation, $1 \leq i \leq \frac{K!}{3!}$!, also called the *$i^{th}$-tessellated calibration*. Each ω^i belongs to set of all possible calibrations $\Omega(\mathbf{t})$, which have interesting properties that are described in the rest of the section.

3.1 Representation of Calibration Sets

For a given display system with K primaries, it can be shown that any convex combination of calibrations for a color $\mathbf{t}$ are also calibrations, that is $\Omega(\mathbf{t})$ is a convex set. Moreover, since elements in the calibration set satisfy three linear equations corresponding to the tristimulus constraints, the calibration set can be interpreted as the intersection of bounded hyperplanes, defined by tristimulus constraints, and in this way, it can be shown that the calibration set is a polytope[2], which is expressed as the following theorem.

Theorem 3.1 *For a color $\mathbf{t} \in \mathscr{G}$, the calibration set $\Omega(\mathbf{t})$ is a convex polytope.*

From Theorem 3.1, we have that the calibration set is the convex hull of a finite set of calibrations, which are also the vertices of the convex set. In fact, using convexity and considering that the calibration set is bounded by the hypercube, it possible to show that the tessellated calibrations are the vertices of the polytope and therefore, the following lemma follows,

Lemma 3.2 *An extreme point of calibration set $\Omega(\mathbf{t})$ is a tessellated calibration.*

Since the tessellation calibrations are the extreme points of the polytope $\Omega(\mathbf{t})$, and by definition, a convex polytope is the convex hull of a finite set of points, a direct consequence of these facts is the following theorem that characterizes the set of calibrations.

Theorem 3.3 (Representation) *For a given color $\mathbf{t} \in \mathscr{G}$, with calibration set $\Omega(\mathbf{t})$ and tessellated calibrations $\omega^1, \omega^2, \ldots, \omega^{\frac{K!}{3!}}$, the set of calibrations is the convex hull of the tessellated calibrations, i.e.,*

$$\Omega(\mathbf{t}) = conv\left\{\omega^1, \omega^2, \ldots, \omega^{\frac{K!}{3!}}\right\}. \tag{8}$$

[2]The convex hull of a finite set of vectors $\alpha_1, \ldots, \alpha_N$ in $\mathbb{R}^K$, is called a *convex polytope* [18].

As already noted in Section 2.2 not all of the $\frac{K!}{3!}$ potential tessellations of the gamut are distinct and therefore the result in (8) can alternatively be written as

$$\Omega(\mathbf{t}) = \text{conv}\left\{\omega^{j_1}, \omega^{j_2}, \ldots, \omega^{j_{N_T}}\right\}. \tag{9}$$

where N_T is the number of distinct tessellations and $j_1, j_2, \ldots j_{N_T}$ is a set of indices that selects these distinct tessellations from among the $\frac{K!}{3!}$ potential options.

4 Subspace Decomposition of the Display Control Space

The representation of calibration sets in the K dimensional device control space covered in the preceding section, although useful, is not immediately conducive to visualization because $K \geq 4$ for multiprimary displays. In this section, we show that a suitable subspace decomposition of the device control space alleviates this problem and also offers advantages in terms of analysis of alternative calibration strategies.

Consider the $K \times 3$ matrix $\mathbf{A} = \mathbf{P}^T$ which has the primary tristimulus values as its rows. The tristimulus value corresponding to a control vector α can then be written as

$$\mathbf{t} = \mathbf{P}\alpha + \mathbf{t}_0 = \mathbf{A}^T\alpha + \mathbf{t}_0. \tag{10}$$

The entries in the columns of $\mathbf{A}^T\alpha$ correspond to the inner products between the columns of $\mathbf{A}$ and control vector α and therefore this computation is equivalent to the projection of the control vector α onto the column space of $\mathbf{A}$ [19]. The control vectors α lie in the vector space $\mathbb{R}^K$ formed by K-tuples of real values. Via the orthogonal decomposition theorem [20, pp. 405], this space can be decomposed as

$$\mathbb{R}^k = \mathscr{R}(\mathbf{A}) + \mathscr{N}\left(\mathbf{A}^T\right) = \mathscr{R}(\mathbf{A}) + \mathscr{N}(\mathbf{P}), \tag{11}$$

where $\mathscr{R}(\mathbf{A})$ is the range of $\mathbf{A}$, i.e., the subspace spanned by the columns of $\mathbf{A}$ and $\mathscr{N}\left(\mathbf{A}^T\right) = \mathscr{N}(\mathbf{P}) \stackrel{\text{def}}{=} \left\{\beta \mid \mathbf{A}^T\beta = \mathbf{0}\right\}$ is the null space of $\mathbf{A}^T = \mathbf{P}$ and the orthogonal complement of $\mathscr{R}(\mathbf{A})$ in $\mathbb{R}^k$. We refer to $\mathscr{R}(\mathbf{A}) = \mathscr{R}\left(\mathbf{P}^T\right)$ as the *control visual subspace (CVS)* and to $\mathscr{N}\left(\mathbf{A}^T\right) = \mathscr{N}(\mathbf{P})$ as the *control black subspace (CBS)* drawing upon the analogy with the human visual subspace and the metameric black subspace [21, 22].

Now observe that if α_1 and α_2 are two control values that yield the same tristimulus $\mathbf{t}$, i.e., they lie in the calibration set corresponding to $\mathbf{t}$, then from (10), we immediately see that

$$\mathbf{A}^T(\alpha_1 - \alpha_2) = \mathbf{0}, \tag{12}$$

and therefore the variations in calibration sets are contained entirely within the CBS. The calibration sets can therefore be visualized in the CBS. In particular, suppose that $\mathbf{V} = [\mathbf{v}_1, \mathbf{v}_2, \mathbf{v}_3]$ is a $K \times 3$ matrix whose columns $\mathbf{v}_i, i = 1, 2, 3$ form an orthonormal basis for the column space of $\mathbf{A}$ and $\mathbf{B} = \left[\mathbf{b}_1, \mathbf{b}_2, \ldots \mathbf{b}_{(K-3)}\right]$ is a $K \times (K-3)$ matrix whose columns $\mathbf{b}_i, i = 1, 2, \ldots (K-3)$ form an orthonormal basis for $\mathscr{N}\left(\mathbf{A}^T\right) = \mathscr{N}(\mathbf{P})$. Then (11) implies that

$$\alpha = \mathbf{V}\mathbf{V}^T\alpha + \mathbf{B}\mathbf{B}^T\alpha. \tag{13}$$

It can be seen that for any point in the calibration set $\Omega(\mathbf{t})$

$$\mathbf{V}\mathbf{V}^T\alpha = \mathbf{P}^T\left(\mathbf{P}\mathbf{P}^T\right)^{-1}\mathbf{t} \tag{14}$$

and therefore this component is constant for all points in $\Omega(\mathbf{t})$. The set $\Omega(\mathbf{t})$ is therefore contained entirely in a linear variety, i.e., a translated version of, the CBS. Variations in $\Omega(\mathbf{t})$ can be represented and visualized completely in terms of the $(K-3)\times 1$ coordinate vector $\beta = \mathbf{B}^T\alpha$. In particular, the polytope vertices $\omega^1, \omega^2, \ldots, \omega^{\frac{K!}{3!}}$ that define $\Omega(\mathbf{t})$ can all be expressed as

$$\omega^j = \mathbf{P}^T\left(\mathbf{P}\mathbf{P}^T\right)^{-1}\mathbf{t} + \mathbf{B}\mathbf{B}^T\omega^j = \mathbf{P}^T\left(\mathbf{P}\mathbf{P}^T\right)^{-1}\mathbf{t} + \mathbf{B}\beta_\omega^j. \tag{15}$$

and therefore

$$\Omega(\mathbf{t}) = \mathbf{P}^T\left(\mathbf{P}\mathbf{P}^T\right)^{-1}\mathbf{t} + \mathbf{B}\Xi(\mathbf{t}), \tag{16}$$

where $\beta_\omega^j = \mathbf{B}^T\omega^j, j = 1,2,\ldots\frac{K!}{3!}$, and

$$\Xi(\mathbf{t}) = \mathrm{conv}\left\{\beta_\omega^1, \beta_\omega^2, \ldots, \beta_\omega^{\frac{K!}{3!}}\right\} \tag{17}$$

$$= \mathrm{conv}\left\{\beta_\omega^{j_1}, \beta_\omega^{j_2}, \ldots, \beta_\omega^{j_{N_T}}\right\}. \tag{18}$$

is a convex polytope in $\mathbb{R}^{(K-3)}$, a $(K-3)$ dimensional coordinate representation for the CBS in terms of the basis $\mathbf{B}$.

Note that because intervals are the only possible polytopes in one-dimensional space, we have the following theorem.

Theorem 4.1 *For a given color $\mathbf{t}\in\mathscr{G}$, of a four primary display, there are at most two distinct tessellated calibrations.*

The proposed subspace decomposition is particularly useful because it decomposes the K dimensional space of control values that define the displayed color into the 3 dimensional CVS that is completely determined by the requested colorimetry and the $(K-3)$ dimensional CBS that is unconstrained by the colorimetry requirements and only subject to bounds due to the feasibility limits on the space of control values. As outlined above, coupled with the polytope representation developed for the calibration set in the previous section, the decomposition completely characterizes the flexibility in the choice of the calibration for a color as a polytope in a linear variety of the CBS. Since there is no flexibility in the choice of the CVS component, alternative calibration strategies differ only with respect to their CBS components lying in the polytopes $\Xi(\mathbf{t})$, which can be conveniently be visualized as $1,2$, and 3 dimensional representations, respectively, for $K = 4,5$, and 6. For $K \geq 7$, whereas the sets cannot be readily visualized the intuition and analysis methodology developed can still be exploited for the formulation and analysis of alternative calibration strategies.

A calibration specification over the entire gamut is obtained by choosing a specific calibration $\alpha(\mathbf{t})$ for each color in the entire gamut, i.e., for each $\mathbf{t}\in\mathscr{G}$. In the ideal situation, the calibrations $\Omega(\mathbf{t})$ all produce the same color and therefore one may select among these, arbitrarily or based on another criterion, to obtain $\alpha(\mathbf{t})$, and the choice at each point $\mathbf{t}$ in the gamut can be made independently of any other point in the gamut. In practice, however, defining $\alpha(\mathbf{t})$ via a random selection from $\Omega(\mathbf{t})$ at each $\mathbf{t}$ is not acceptable because of device variations and observer variations that cause deviations from the ideal mathematical model of (2). Specifically, if the calibration specification $\alpha(\mathbf{t})$ is not continuous (and smooth) over the entire space of in gamut colors $\mathbf{t}\in\mathscr{G}$, input images that have continuous and smooth spatial variations in color spanning the color space regions with calibration discontinuities exhibit as artifacts discontinuities and non-smooth variations in the images rendered by the display (induced by the device and observer variability). For this reason, it is desirable to also choose the calibration $\alpha(\mathbf{t})$ to be continuous and smooth function of the color $\mathbf{t}$ for $\mathbf{t}\in\mathscr{G}$. The proposed approach using the decomposition of the display control space into the CVS and the CBS also allows us to visualize and analyze the behavior of a specific calibration $\alpha(\mathbf{t})$ specified over the entire gamut $\mathbf{t}\in\mathscr{G}$ over various trajectories in color space. Specifically, because the CVS component of $\alpha(\mathbf{t})$ is completely determined by the colorimetry and because the basis vectors in $\mathbf{B}$ are orthonormal, the variation in $\alpha(\mathbf{t})$ exactly corresponds to the variation in $\beta(\mathbf{t}) = \mathbf{B}^T\alpha(\mathbf{t})$, where the latter is conveniently represented and visualized in the $(K-3)$ dimensional space $\mathbb{R}^{(K-3)}$ in terms of the bases $\mathbf{B}$. Specifically, for $K = 4$ and $K = 5$, the functions $\beta(\mathbf{t})$ can be visualized as 2 or 3 dimensional plots, respectively, for any chosen one dimensional trajectory for $\mathbf{t}$ in the color space. Plotting the corresponding sets $\Xi(\mathbf{t})$ that characterize the flexibility in the calibration on the same plot helps to also identify the available leeway in the choice of calibration in order to meet the smoothness requirement. In the following subsection, we illustrate these ideas concretely, by building further upon our example of Section 2.2.

	Tessellation 1	Tessellation 2
$\omega(\mathbf{t})$	$[0.1164, 0.3658, 0, 0.2545]^T$	$[0.2529, 0, 0.3710, 0.1128]^T$
β	0.2765	-0.2805

Table 1. The two calibrations corresponding to the alternative gamut tessellations for the system with $K = 4$ primaries defined in (5) for a color $\mathbf{t} = [0.1178, 0.1620, 0.1192]^T$, which is located on the luminance axis with $L^* = 50$, and chromaticity values $u^* = v^* = 0$. The calibration set $\Omega(\mathbf{t})$ consists of the line segment between these two extremal calibrations and is contained within a linear variety of the $(K-3) = 1$ dimensional black space spanned by $\mathbf{B} = [-0.2452, 0.6568, -0.6662, 0.2545]^T$. The set $\Xi(\mathbf{t})$ corresponds to the interval $[-0.2805, 0.2765]$.

4.1 Calibration Set Visualization Example

As an example, consider the four primary system defined in (5). Since $K = 4$, the CBS is one dimensional; it can be seen that $\mathbf{B} = [-0.2452, 0.6568, -0.6662, 0.2545]^T$ is a basis for the CBS. The system has two alternative tessellations of the gamut discussed in Section 2.2 and shown in Fig. 2. Table 1 lists the two alternative calibrations for the color $\mathbf{t}$, located on the luminance axis with $L^* = 50$, and chromaticity values $u^* = v^* = 0$. The set $\Omega(\mathbf{t})$ is the line segment between these extremal calibrations in $\mathbb{R}^4$ and corresponds to a linear variety of the CBS and in terms of the basis $\mathbf{B}$ is represented by the set $\Xi(\mathbf{t}) = [-0.2805, 0.2765]$, a one-dimensional interval.

As described in the preceding section, the visualization is also be useful for examining the smoothness of a specific calibration $\alpha(\mathbf{t})$ specified over the entire gamut $\mathbf{t}\in\mathscr{G}$, along specific trajectories in color space. Specifically, for our example, since $\Xi(\mathbf{t})$ is a one dimensional set, we can use other dimensions in a

graphical representation to visualize calibrations, and properties of the calibrations that are not purely a function of the colorimetry. As a specific example, consider the trajectory along the luminance axis, L^*, with chromaticity coordinates $u^* = v^* = 0$. Figure 4(a)(a) shows along the ordinate, visualizations of the "calibration flexibility" sets $\Xi(\mathbf{t})$ as a function of L^* along this trajectory samples in steps of 10 L^* units. We can appreciate that for $L^* = 0$ and $L^* = 100$, the calibration set corresponds to a point. This is expected, since both points belong to the gamut boundary, where the calibration is unique [23] and there is no flexibility in the choice of calibration. At other L^* values, the width of the interval $\Xi(\mathbf{t})$ represents the available flexibility in calibration in terms of distance in control space and one sees that this flexibility is the maximum at an L^* close to 80 and decreases on either side as L^* increases or decreases. Similarly, the sets $\Xi(\mathbf{t})$ are shown in Fig. 4(b)(b) for points located along the u^* axis at $L^* = 70$ and $v^* = 0$. In this case, one sees that the calibration flexibility is fairly constant across a wide range of u^* values and drops rapidly as one approaches the extremal values. Subsequently in Section 6 we will see how these visualizations can be further augmented to examine specific calibration strategies.

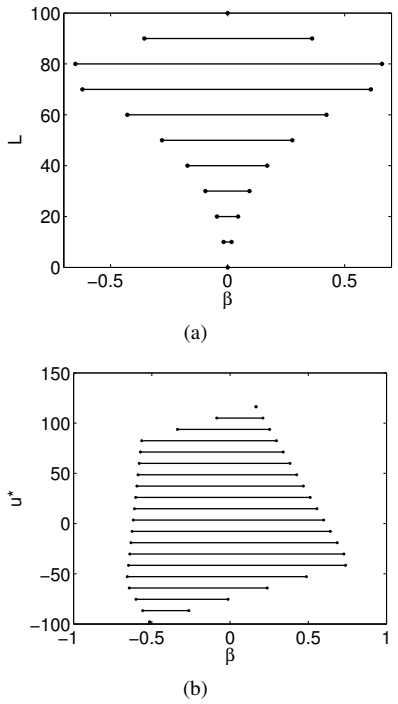

Figure 4. *Visualization of $\Xi(\mathbf{t})$ for the four primary defined in (5) for colors $\mathbf{t}$ chosen along two one-dimensional trajectories chosen along the axes in CIELUV space: (a) Colors $\mathbf{t}$ located on the luminance axis L^*, with constant chromaticity $u^* = v^* = 0$, (b) Colors $\mathbf{t}$ located along the u^* axis, with $L^* = 70, v^* = 0$.*

5 Optimal Power Calibrations

Theorem 3.3 provides a concrete characterization for the calibration sets. Based on this is possible to analyze performance variation due to different choices of calibrations. As an example, we consider in this section the optical power of a display system as a criteria of performance, and offer a characterization for the calibrations that consume the minimal and maximal optical power.

5.1 Optical Power in Multiprimary systems

Let denote by ϕ_k the optical power for the k^{th} primary, $1 \leq k \leq K$, when it is displayed at full intensity, which can be expressed as,

$$\phi_k = \int_\lambda p_k(\lambda) d\lambda \tag{19}$$

The total optical power emitted when he display is driven by a set of control signal α is denoted by $\varphi(\alpha)$

$$\begin{aligned} \varphi(\alpha) &= \sum_{k=1}^{K} \alpha_k \phi_k + \phi_0, \\ &= \phi_{\mathbf{P}}^T \alpha + \phi_0, \end{aligned} \tag{20}$$

where $\phi_{\mathbf{P}}$ is the primary optical power vector $\phi_{\mathbf{P}} = [\phi_1, .., \phi_K]^T$, and ϕ_0 is the optical power of the black spectral radiance.

5.2 Optimal Power Calibrations

In contrast to the color perception, where different calibrations for the same color provides the same color sensation, optical power is clearly affected by different choices of calibration. Since there is a proportional relationship between optical power and the electrical power consumed, calibrations for minimum optical power are often considered desirable.

For a given color $\mathbf{t} \in \mathscr{G}$, the minimum power that can be used for its reproduction is denoted by $\varphi_{min}(\mathbf{t})$, and it is achieved by a calibration $\alpha_{min} \in \Omega(\mathbf{t})$ that solves the following optimization problem,

$$\varphi_{min} = \min_{\alpha \in \Omega(\mathbf{t})} \phi_{\mathbf{P}}^T \alpha, \tag{21}$$

which is a problem defined over a convex region $\Omega(\mathbf{t})$. Since the function to minimize is a linear function, the optimization in (21) is also a linear programing problem, which optimal solutions are located on the vertices of the polytope [24], demonstrating the following theorem:

Theorem 5.1 *For a given color $\mathbf{t} \in \mathscr{G}$ with tessellated calibrations $\omega^1, \ldots, \omega^{\frac{K!}{3!}}$, the minimum optical power $\varphi_{min}(\mathbf{t})$ that can be achieved to reproduce $\mathbf{t}$ is,*

$$\varphi_{min}(\mathbf{t}) = \min_{i=1,\ldots,\frac{K!}{3!}} \left\{ \phi_{\mathbf{P}}^T \omega^i \right\}. \tag{22}$$

Theorem 5.1 implies that the optimal solution is obtained by one of the tessellated calibrations ω^i. Although multiple calibrations may be optimal, a unique calibration selection can be assured by ordering the $\frac{K!}{3!}$ tessellations and selecting the optimal calibration with the lowest index. In this way, a minimum power calibration $\alpha_{min}(\mathbf{t})$, is defined to be

$$\alpha_{min}(\mathbf{t}) = \omega^j, \; s.t. \; j = \arg \min_{i=1,2\ldots,\frac{K!}{3!}} \left\{ \omega^i \,\middle|\, \phi_{min} = \phi_{\mathbf{P}}^T \omega^i \right\}. \tag{23}$$

Equations (22) and (23) allow us to formulate an algorithm to compute uniquely color calibrations for the minimum optical power consumption[3].

Expressions similar to (22) and (23) can also be formulated to define the maximum power $\varphi_{max}(\mathbf{t})$ and the maximum power calibration α_{max} from which we conclude that one of the tessellated calibrations ω^i attains the maximal power.

To visualize the optimal power strategy, consider once again tone variations along the luminance axis with L^*, and chromaticity values $u^* = v^* = 0$, for colors reproduced by the system in (5). Figure 5(a) shows the visualization of the calibration sets for different luminance values. It also shows the calibration transition by considering the minimum power strategy (the line plotted in blue) and the maximum power (red line). It can be appreciated how each strategy takes one of the vertexes of calibration sets. The smoothness in the transitions depends exclusively on the size and location of the calibration sets. In addition to the minimum and maximum power, we define the mean power calibration as,

$$\alpha_{mean}(\mathbf{t}) = \frac{1}{N_T}\sum_{i=1}^{N_T} \omega^{j_i}, \tag{24}$$

which is plotted in magenta in Fig. 5. For each of the strategies, Fig. 5(b) also shows the gray calibration "TRC curves" are also shown as plots individual control values $\alpha_i, i = 1,2,3,4$ as a function of L^* along the gray axes. It can be seen how for this particular example the curves for optimal power offer non-smooth transitions at some color values, while the average strategy offers smooth transitions. These observations correlates with with those from Fig. 5

6 Results

Having formulated the methodology for the representation and visualization of calibration sets and specific calibrations, in this section, we consider application of the methodology to systems with $K = 4,5,6$ primaries. In order to have reasonable and meaningful designs of these multiprimary systems (as opposed to random selections), we consider specifically the multiprimary designs obtained in [5] where the deviation of the CIELUV gamut from optimal color gamut was minimized under an overall optical power constraint. The parameters of the corresponding systems can be obtained from [5].

As a first step, we consider the color $\mathbf{t}$ located on the luminance axis with $L^* = 50$, and chromaticity values $u^* = v^* = 0$. For each display system we compute the tessellated calibrations and, in Fig. 6, visualize the set $\Xi(\mathbf{t})$ based on the proposed subspace decomposition. For $K = 4,5$, and 6, the sets $\Xi(\mathbf{t})$ are, respectively, a line segment, a convex polytope in a 2-D plane, and a convex polytope in a three-dimensional space.

We also consider the calibrations for color trajectories corresponding to tone transitions along the luminance axis, L^* ($u^* = v^* = 0$), and the chromaticity axes u^* ($L^* = 70, v^* = 0$) and v^*

[3] An analogous result has recently also been derived independently by Centore [25] adopting a different approach that does not obtain or rely on the complete characterization of calibration sets for multiprimary displays. The minimum optimal power calibration problem has also been previously proposed in [13] where the optimization was performed numerically without the benefit of the proposed representation for the calibration sets.

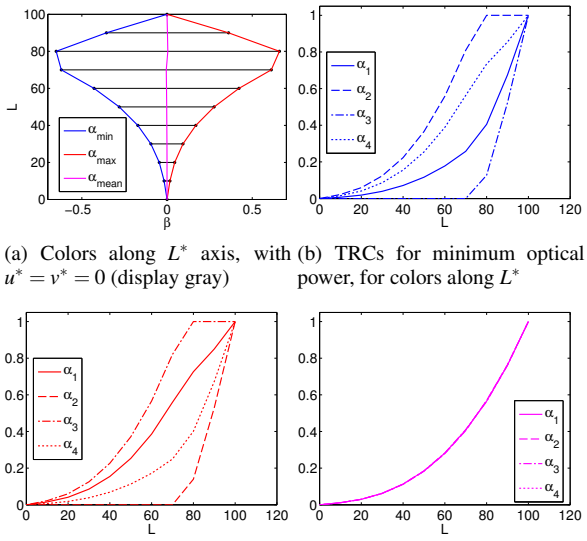

(a) Colors along L^* axis, with $u^* = v^* = 0$ (display gray)

(b) TRCs for minimum optical power, for colors along L^*

(c) TRCs for minimum optical power, for colors along L^*

(d) TRCs from mean of calibrations, for colors along L^*

Figure 5. *Top left: Visualization of $\Xi(\mathbf{t})$, for a colors $\mathbf{t}$ on the luminance axis L^* ($u^* = v^* = 0$), displayed by the 4 primary system in (5). On top of the figure, a representation for different calibration strategies are plotted. The blue line contains the calibrations for minimal and maximal optical power, the red on red has the maximum power strategy. The averaging strategy is presented in magenta. The remaining figures show the actual calibration values for each of the strategies.*

($L^* = 70, u^* = 0$). Figure 7(a)shows the visual representation for the sets $\Xi(\mathbf{t})$, for colors sampled along the luminance axis at a spacing of $10\Delta E$ units, when they are reproduced by the four primary system. Note that size for the calibration representation sets varies with respect the luminance value. Bigger sets provides more flexibility for choosing a particular calibration. This plot has been overlaid with four different colored lines representing four alternative calibration strategies: minimum, and maximal optical power, mean calibration, and matrix switching (MS) [11]. Each of the calibration approaches maintains continuity of the calibration transformation $\alpha(\mathbf{t})$ as a function of $\mathbf{t}$ (at the points shown and at other points). Note, however, that the strategies based on minimizing or maximizing optical power and the strategy based on averaging does not provide smooth transitions in the device control space; derivative discontinuities are immediately apparent for these strategies in Fig. 7(a). The MS method offers the smoothest transition among the tested methods, and the calibrations are located toward the center of $\Xi(\mathbf{t})$, implying medium power consumption. However, these assessments are not valid in general. Figures 7(b) and 7(c) show the sets $\Xi(\mathbf{t})$ for colors on the u^* and v^* axes, respectively. In these figures, it can be appreciated that the MS methodology also presents derivative discontinuities, and for the case of the u^* axis, the power consumption is closer to the maximum power, specially for desaturated colors.

For these examples, the visualization methodology also makes evident that smoother calibration paths are feasible for the set of calibrations, which are are not considered by the evaluated methodologies. Is important to note that the flexibility for choosing the calibrations is dependent upon location in color space.

This is more evident when we consider a tone transition from black to white, with $v^* = 0$, and which u^* component at 85% of the maximum CIELUV chroma for in-gamut colors. The visualization for sets $\Xi(\mathbf{t})$ are shown in Fig. 7(d)(d) for this case, where it is evident that the widths of the calibration sets are narrower than in Fig. 7(d)(a). In this case, the matrix switching provides calibrations similar to the maximum power strategy, which also seems to offer the smoothest transition.

Figure 8 shows the sets $\Xi(\mathbf{t})$ for colors on the luminance and u^* axes, when reproduced by the five primary display. It is clear that having more primaries increases the flexibility for determining calibrations. Note in this figure how the MS methodology offer the smoothest transitions along the gray axis, but fails to preserve smoothness along the chromatic axes.

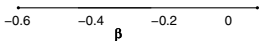

(a) $K = 4$

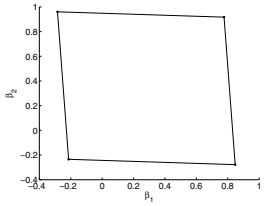

(b) $K = 5$

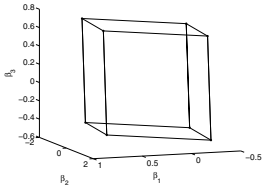

(c) $K = 6$

Figure 6. *Visualization of the convex polytopes $\Xi(\mathbf{t})$, for a color $\mathbf{t}$ located on the luminance axis with $L^* = 70$, and chromaticity values $u^* = v^* = 0$, for display systems with primaries $K = 4,5,6$. The calibrations sets are polytopes lie on $K-3$ dimensional subspaces, and their vertexes correspond to the tessellated calibrations.*

7 Discussion and Conclusions

We have presented a theoretical characterization of the set of calibrations for a multiprimary display, as the convex hull of tessellated calibrations. This characterization has important consequences. First, it directly leads to a characterization and method of computation for the optimal power calibration and also allows formulation of other criteria in a convex optimization framework. Second by using a suitable decomposition of the display control space that we also propose here, the representation allows effective visualization and analysis of the flexibility available in calibration in different parts of color space and the behavior of a chosen calibration strategy along a chosen trajectory in color space with regard to smooth transitions in device space and in the context of the calibration flexibility. Using the proposed methodology, we studied prototypical multiprimary systems designed with four and five primaries and showed that the optimal power calibration strategies and the matrix switching methodology previously

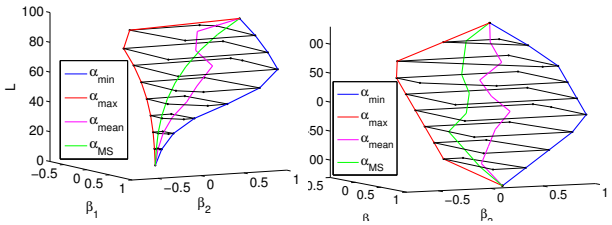

(a) (b)

Figure 8. *On the top left, the visualization of the set $\Xi(\mathbf{t})$, Visualization of $\Xi(\mathbf{t})$ for colors varying on two different perceptual regions. Top: colors located on the u^* axis, with $L^* = 70, v^* = 0$ (top figures). Bottom: colors on the v^* axis, with constant $L^* = 70, u^* = 0$. The sets is shown for system with $K = 4$ primaries (left) and $K = 5$ (right). The figure also presents a representation of the calibration strategies for minimal (α_min) and maximal optical power(α_max), in blue and red colors respectively. It also shows the average strategy (α_mean) in magenta, and the matrix switching (α_MS) in green.*

proposed in the literature exhibit significant non-smooth behavior in different parts of color space. The results indicate that practical calibration strategies for multiprimary displays require a trade-off between the objectives of minimizing power and of robustness to device and observer variations and that further work using alternative formulations, some of which may be enabled by the proposed framework, is necessary to develop effective strategies for calibration.

To obtain better robustness to device and observer variations, it is important to emphasize smoothness of the calibration as a function of spatial neighborhood in color space. We note that the convex polytope formulation of the space of calibrations readily lends itself to a approaches that formulate the calibration as a convex programming problem where a convex metric is utilized for the smoothness. For example, a variational formulation for color calibration can be obtained by posing the problem of calibration as one of minimizing the energy functional

$$\int_{\mathbf{t}\in\mathscr{G}} \left\| \nabla^2 \alpha(\mathbf{t}) \right\| d\mathbf{t} \tag{25}$$

subject to the constraint that $\alpha(\mathbf{t}) \in \Omega(\mathbf{t})$, which via the proposed formulation maps to a relatively simpler problem

$$\int_{\mathbf{t}\in\mathscr{G}} \left\| \nabla^2 \beta(\mathbf{t}) \right\| d\mathbf{t} \tag{26}$$

subject to the constraint that $\alpha(\mathbf{t}) \in \Xi(\mathbf{t})$. Standard variational methods can be used to numerically obtain a solution to this problem and such approaches offers promising directions for further investigation of alternatives for multiprimary display color calibration.

References

[1] S. Wen, "Design of relative primary luminances for four-primary displays," *Displays*, vol. 26, no. 4-5, pp. 171 – 176, 2005.

[2] ——, "A method for selecting display primaries to match a target color gamut," *Journal of the Society for Information Display*, vol. 15, p. 1015, 2007.

[3] H. Cheng, I. Ben-David, and S. Wu, "Five-Primary-Color LCDs," *Journal of Display Technology*, vol. 6, no. 1, pp. 3–7, 2010.

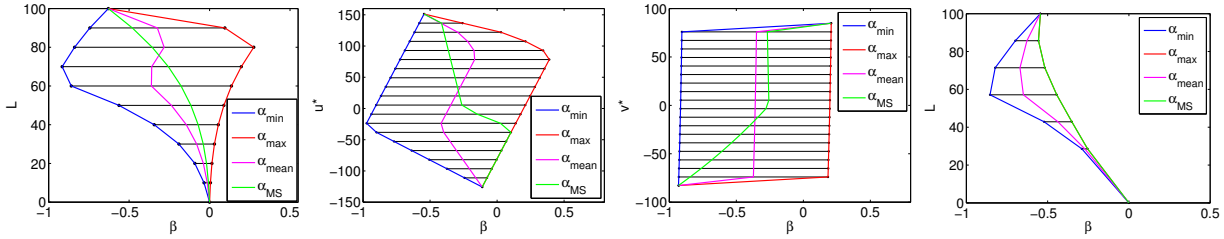

Figure 7. *Visualization of calibration sets $\Omega(\mathbf{t})$, for a colors $\mathbf{t}$ for three different tone variations. located on the gray level with constant chromaticity $u^* = v^* = 0$, and displayed by a 4 primary system. The figure also presents a representation of the calibration strategies for minimal and maximal optical power, blue and red respectively, and also the strategy of averaging the tessellated calibrations.*

[4] C. E. Rodríguez-Pardo, G. Sharma, X. Feng, J. Speigle, and I. Sezan, "Optimal gamut volume design for three primary and multiprimary display systems," in *Proc. SPIE: Color Imaging XVII: Displaying, Hardcopy, Processing, and Applications*, R. Eschbach, G. G. Marcu, and A. Rizzi, Eds., vol. 8292, Jan. 2012, pp. 8292–0C,1–7.

[5] C. Rodríguez-Pardo, G. Sharma, and X.-F. Feng, "Primary selection for uniform display response," in *Proc. SPIE: Color Imaging XIX: Displaying, Processing, Hardcopy, and Applications*, R. Eschbach, G. G. Marcu, and A. Rizzi, Eds., vol. 9015, Feb. 2014, pp. 90 150I–1–90 150I–9.

[6] K. Yoshiyama, M. Teragawa, A. Yoshida, K. Tomizawa, K. Nakamura, Y. Yoshida, and Y. Yamamoto, "Power-saving: A new advantage of multi-primary color displays derived by numerical analysis," in *SID Symposium Digest of Technical Papers*, vol. 41, May 2010, pp. 416–418.

[7] C.-C. Tsai, F.-C. Lin, Y.-P. Huang, , and H.-P. D. Shieh, "RGBW 4-in-1 LEDs for backlight system for ultra-low power consumption field-sequential-color LCDs," in *SID Symposium Digest of Technical Papers*, vol. 41, May 2010, pp. 420–423.

[8] S. Ueki, K. Nakamura, Yuhichi, Yoshida, T. Mori, K. Tomizawa, Y. Narutaki, Y. Itoh, , and K. Okamoto, "Five-Primary-Color 60-inch LCD with novel wide color gamut and wide viewing angle," in *SID Symposium Digest of Technical Papers*, vol. 40, June 2009, pp. 927–930.

[9] K. Tomizawa, K. Nakamura, S. Ueki, Y. Yoshida, T. Mori, M. Hasegawa, A. Yoshida, Y. Narutaki, Y. Itoh, Y. Yoshida *et al.*, "Multi-primary-color LCD: Its characteristics and extended applications," *Journal of the Society for Information Display*, vol. 19, no. 5, pp. 369–379, 2011.

[10] M. Teragawa, A. Yoshida, K. Yoshiyama, S. Nakagawa, K. Tomizawa, and Y. Yoshida, "Review paper: Multi-primary-color displays: The latest technologies and their benefits," *Journal of the Society for Information Display*, vol. 20, no. 1, pp. 1–11, 2012.

[11] T. Ajito, K. Ohsawa, T. Obi, M. Yamaguchi, and N. Ohyama, "Color conversion method for multiprimary display using matrix switching," *Optical Review*, vol. 8, no. 2, pp. 191–197, 2001.

[12] Y. Murakami, N. Hatano, J. Takiue, M. Yamaguchi, and N. Ohyama, "Evaluation of smooth tonal change reproduction on multiprimary display: comparison of color conversion algorithms," in *Proc. SPIE: Color Imaging X: Processing, Hardcopy, and Applications*, L. C. Chien and M. H. Wu, Eds., vol. 5289, Jan. 2004, pp. 275–283.

[13] M. Takaya, K. Ito, G. Ohashi, and Y. Shimodaira, "Color-conversion method for a multi-primary display to reduce power consumption and conversion time," *Journal of the Society for Information Display*, vol. 13, no. 8, pp. 685–690, 2012.

[14] C. E. Rodríguez-Pardo, G. Sharma, J. Speigle, X. Feng, and I. Sezan, "Efficient computation of display gamut volumes in perceptual spaces," in *Proc. IS&T/SID Nineteenth Color and Imaging Conference: Color Science and Engineering Systems, Technologies, and Applications*, San Jose, CA, 7-11 Nov. 2011, pp. 132–138.

[15] P. Centore and M. H. Brill, "Extensible multi-primary control sequences," *Journal of the Society for Information Display*, vol. 20, no. 1, pp. 12–21, 2012.

[16] G. Sharma and C. Rodríguez-Pardo, "Geometry of Multiprimary Display Colors: Gamut and Calibration," In preparation, 2014.

[17] CIE, "Colorimetry," CIE Publication No. 15.2, Central Bureau of the CIE, Vienna, 1986, the commonly used data on color matching functions is available at the CIE web site at http://www.cie.co.at/.

[18] S. R. Lay, *Convex sets and their applications*. Malabar, FL: Krieger Publishing Company, 1992.

[19] A. W. Naylor and G. R. Sell, *Linear Operator Theory in Engineering and Science*. Berlin: Springer-Verlag, 1982.

[20] C. Meyer, *Matrix analysis and applied linear algebra*. Philadephia, PA: Society for Industrial and Applied Mathematics, 2000.

[21] G. Sharma and H. J. Trussell, "Digital color imaging," *IEEE Trans. Image Proc.*, vol. 6, no. 7, pp. 901–932, Jul. 1997.

[22] J. B. Cohen, Ed., *Visual Color and Color Mixture: The Fundamental Color Space*. Urbana, IL: University of Illinois Press, 2001.

[23] P. Centore, "Non-metamerism of boundary colors in multi-primary displays," *Journal of the Society for Information Display*, vol. 20, no. 4, pp. 214–220, 2012.

[24] D. G. Luenberger, *Linear and Nonlinear Programming*, 2nd ed. Reading, MA: Addison Wesley, 1989.

[25] P. Centore, "Minimal-energy multi-primary control sequences," personal communication, received from the author 27 Apr. 2014.